

INTRODUCTION

Artificial surface textures affect the tribological characteristics of lubricated contacts and, if designed properly, are capable of enhancing the performance of hydrodynamic bearings [1]. Under hydrodynamic conditions the desired effects are generally a reduction in frictional losses and an increase in minimum film thickness for a safer and more efficient bearing operation. Under mixed or starved lubrication conditions, e.g. during start-up, textures may act as lubricant reservoirs or trap wear debris, therefore potentially reducing wear and limiting bearing failure.

Although promising results are being reported, successful applications are still very limited. As the impact of texturing highly depends on the contact geometry and operating conditions (film shape and thickness, lubricant viscosity, rotational speed etc.), designing optimized texture patterns in terms of their geometrical parameters (shape, size, distribution) is a challenging task. A poorly designed texture pattern may even cause a deterioration in bearing performance, further underlining the importance of a thorough texture design. Accurate and robust computational models are therefore crucial, however, high computation times are usually encountered due to the fine meshes required to accurately capture the complex geometry, the need for mass-conserving cavitation models and the presence of multiple discontinuities in the film thickness equation.

In the present work, a fast numerical model based on the Reynolds equation is applied to study partially textured tilting pad thrust bearings (see Fig. 1). The computation time of the numerical model is reduced significantly by applying special discretization formulae to handle discontinuities, taking advantage of multicore processing and strategically making use of different solvers to find the bearing equilibrium. A nonlinear constrained optimization utilizing an interior-point algorithm is then performed to optimize texture designs in terms of texture depth, circumferential extend and radial extend.

NUMERICAL MODEL

The film thickness distribution is determined by the film thickness at the pivot (h_p), pitch angle (α_r) and roll angle (α_θ) and can be expressed as follows:

$$h(\theta, r) = h_p + r \sin(\theta_p - \theta) \sin \alpha_r + [r_p - r \cos(\theta_p - \theta)] \sin \alpha_\theta \quad (1)$$

where the texture depth is simply added wherever textures are located. Incorporating mass-conserving cavitation, which may occur inside individual textures close to the pad inlet and the outer radius, the utilized Reynolds equation reads [2]:

$$\frac{\partial}{\partial r} \left(r \frac{\rho h^3}{\eta} \frac{\partial p}{\partial r} \right) + \frac{1}{r} \frac{\partial}{\partial \theta} \left(\frac{\rho h^3}{\eta} \frac{\partial p}{\partial \theta} \right) = 6\omega r \frac{\partial(\theta \rho h)}{\partial \theta} \quad \text{with } p > p_{cav} \text{ for } \theta = 1 \text{ and } p = p_{cav} \text{ for } \theta < 1 \quad (2)$$

where θ is the fractional film content. To extend the validity of the Reynolds equation by considering concentrated inertia effects and reduce computation time, special finite volume discretization formulae are used to discretize the Reynolds equation [3, 4]. Moreover, different mesh sizes are used for the textured and untextured pad areas in order to solve the equations most efficiently. A Gauss-Seidel method with successive relaxation is applied to solve the discrete system, where an additional preceding loop deals with the nonlinearity of the system whenever concentrated inertia effects are considered.

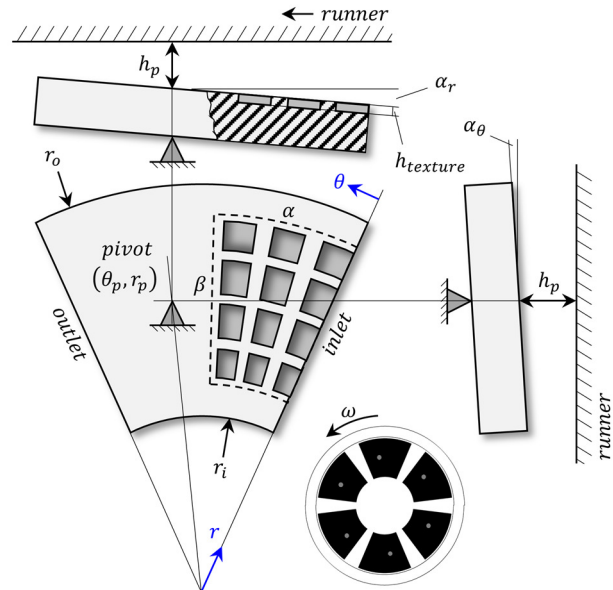


Fig. 1 Tilting pad thrust bearing schematic.

Thermal effects are considered in a simplified manner, applying an iterative effective temperature method [5], while considering the hot-oil-carry-over effect [6]. McCoull and Walther's relation is used to describe the temperature-viscosity relationship [7]. The bearing is in equilibrium when the pad angles and clearance define a film geometry that balances the applied load and causes no resultant moments around the pivot. To find the bearing equilibrium, three methods are implemented and strategically selected based on the residual to reduce the computation time: (i) Newton-Raphson method, (ii) Broyden's method with Sherman-Morrison formula and (iii) continuation method with fourth-order Runge-Kutta technique [8, 9]. To further reduce execution time, Jacobian matrices are evaluated on multiple processor cores and results from the equivalent untextured bearing (pad angles, clearance, temperatures) are used as first approximations for the textured bearing. An empirical damping method is applied to improve the robustness of the equilibrium solver, simply replacing the Jacobian with a *damped Jacobian*: $J_{damped} = (D/k^2 + 1)J$, where k is the iteration number and D the damping parameter (usually $D = 1.5$). Once the equilibrium position, the effective temperature and the pressure distribution are known, the main performance characteristics of the bearing are calculated. The developed model was successfully validated by comparison with CFD data from reference [6], yielding an average error of about 3 % in terms of maximum pressure, friction torque, maximum temperature and minimum film thickness.

TEXTURE DESIGN OPTIMIZATION

The task of optimizing a given texture design involves changing the geometrical parameters of the texture pattern (texture depth, number of textures, size of the textured region, texture density) in order to minimize or maximize a certain bearing performance parameter. In the present work, two single-objective optimization problems are considered, namely maximizing the minimum film thickness (h_{min}) and minimizing the friction torque (T_f).

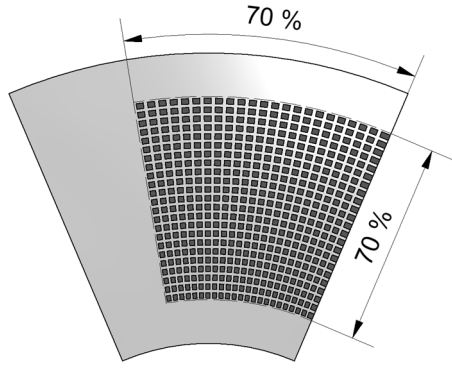


Fig. 2 Exemplary texture design with $h_{texture} = 15 \mu m$, $\alpha = 70 \%$ and $\beta = 70 \%$.

The texture designs considered all consist of angular sector shaped textures with flat bottom profiles as this type of textures has previously been shown to be preferable for converging contacts [1]. It is also known that the texture density cannot be optimized as increasing the density will always improve the performance, meaning that the optimum density is 100 %, which results in a single pocket. However, as a pocket cannot act as a lubricant reservoir during mixed lubrication and the step may wear out quickly, the chosen texture design consists of 23 by 23 textures with a fixed density of 40 % to limit stress concentration on the texture edges (see Fig. 2). This means that three texture design parameters remain for optimization, namely the texture depth ($h_{texture}$), the relative texture extend in circumferential direction (α) and the relative texture extend in radial direction (β). This task can be expressed as a nonlinear constrained optimization problem:

$$\max_x h_{min}(x) \quad \text{such that} \quad x_{min} \leq x \leq x_{max} \quad (3a)$$

$$\min_x T_f(x) \quad \text{such that} \quad x_{min} \leq x \leq x_{max} \quad (3b)$$

where x is a vector containing the texture design parameters, x_{min} and x_{max} define the lower and upper bounds for those parameters, here $0 \leq h_{texture} \leq 50 \mu m$, $10 \leq \alpha \leq 95 \%$ and $10 \leq \beta \leq 95 \%$. All computations are performed on a desktop PC with 16 GB RAM and *Intel Core i7-3770* with four physical cores. Derivatives are evaluated in parallel and a step tolerance value of 10^{-5} is used for x .

RESULTS AND DISCUSSION

Simulations are run for a tilting pad thrust bearing with $r_i = 30.25 \text{ mm}$, $r_o = 70.25 \text{ mm}$ and a pad radius of 46.05° . Pads are supported by a line pivot located at 60 % from the pad inlet. ISO VG 32 oil is supplied at 2 l/min per pad at a constant temperature of 40°C . An average of 30 iterations and 20 minutes of CPU times is required for each optimization. Results are presented in Fig. 3 for three different rotational speeds (1000, 2000 and 3000 rpm) and four specific loads (0.5, 1.0, 1.5 and 2.0 MPa).

It can be seen that the optimum texture depth significantly depends on the operating conditions as well as the optimization objective, ranging from 8 to about $31 \mu m$. The optimum texture depth is on average approximately 10 % lower when the objective is a reduction in friction torque as compared to an increase in minimum film thickness. If the texture depth is related to the respective minimum film thickness ($S = h_{texture}/h_{min}$), relatively constant average optimum values of 0.86 and 0.77 are obtained for an optimization for h_{min} and T_f , respectively, agreeing well with previous findings related to similar contacts [1]. Optimum values for the relative texture extend in circumferential direction are mostly independent from the operating conditions, however, highly depend on the optimization objective. Whereas optimizing for h_{min} results in

values between 68 and 78 %, optimizing for T_f results in much lower values between 46 and 58 %. Optimized relative texture extend in radial direction are fairly independent from the speed and only depend slightly on the applied load and the optimization objective. Optimizing for h_{min} results in values ranging from 58 to 69 % and optimizing for T_f in values ranging from 60 to 73 %.

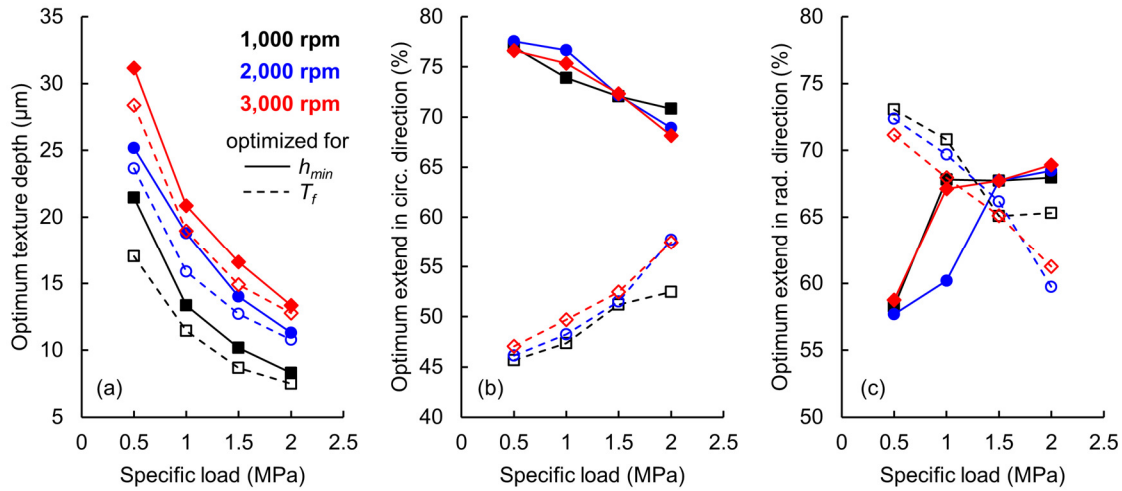


Fig. 3 (a) Optimum texture depth, (b) optimum texture extend in circumferential direction and (c) optimum texture extend in radial direction for different operating conditions and optimization objectives.

It is noteworthy that the texture pattern only influences the bearing performance moderately due to the relatively low selected texture density of 40 %. If optimized for h_{min} , the optimized texture patterns are capable of increasing the minimum film thickness by approximately 6 % as compared to the conventional pads for the operating conditions considered. For these cases the friction torque is hardly influenced by texturing. If the patterns are optimized for T_f , a decrease in friction torque of about 3 % can be achieved. For these cases h_{min} is still increased by an average of 4 %. To achieve a more significant influence of texturing under hydrodynamic conditions, the texture density should be increased as much as possible by using grooves or a pocketed pad design.

CONCLUSIONS

The developed numerical model is successfully used to optimize texture patterns for a line-pivoted tilting pad thrust bearing. The utilized techniques to solve the Reynolds equation and find the load and thermal equilibrium result in low computation times and make it possible to optimize a texture pattern for given load and speed in about 20 min. Whereas optimum values for the size of the textured region are rather independent from the operating conditions, optimum values for the texture depth need to be carefully chosen for the expected range of operating conditions. Experiments are underway on a purposely developed test rig to validate the model and analyze the influence of texturing during start/stop conditions.

ACKNOWLEDGEMENTS

The authors acknowledge the financial support of the Engineering and Physical Sciences Research Council (EPSRC) via grant EP/M50662X/1 and John Crane UK Ltd.

REFERENCES

- [1] Gropper D, Wang L, Harvey TJ. Hydrodynamic lubrication of textured surfaces: A review of modeling techniques and key findings. *Tribology International*. 2016;94:509-29.
- [2] Ausas RF, Ragot P, Leiva J, Jai M, Bayada G, Buscaglia GC. The Impact of the Cavitation Model in the Analysis of Microtextured Lubricated Journal Bearings. *Journal of Tribology*. 2007;129:868-75.
- [3] Dobrica MB, Fillon M. About the validity of Reynolds equation and inertia effects in textured sliders of infinite width. *Proceedings of the Institution of Mechanical Engineers, Part J: Journal of Engineering Tribology*. 2009;223:69-78.
- [4] Arghir M, Alsayed A, Nicolas D. The finite volume solution of the Reynolds equation of lubrication with film discontinuities. *International Journal of Mechanical Sciences*. 2002;44:2119-32.
- [5] Stachowiak GW, Batchelor AW. *Engineering Tribology*. 4th ed. Amsterdam; London: Elsevier/Butterworth-Heinemann; 2014.
- [6] Zouzoulas V, Papadopoulos Cl. 3-D thermohydrodynamic analysis of textured, grooved, pocketed and hydrophobic pivoted-pad thrust bearings. *Tribology International*. 2016.
- [7] Frene J, Nicolas D, Degueurce B, Berthe D, Godet M. *Hydrodynamic Lubrication: Bearings and Thrust Bearings*; Elsevier Science; 1997.
- [8] Burden RL, Faires JD. *Numerical Analysis*; Brooks/Cole, Cengage Learning; 2011.
- [9] Kincaid DR, Cheney EW. *Numerical Analysis: Mathematics of Scientific Computing*; American Mathematical Society; 2002.

NOMENCLATURE

D	damping parameter	T_f	friction torque (Nm)
h	local film thickness (m)	x	vector with texture design parameters
h_{min}	minimum film thickness (m)	x_{max}	upper bounds of x
h_p	film thickness at pivot (m)	x_{min}	lower bounds of x
$h_{texture}$	texture depth (m)	α	relative texture extend in circumferential direction
J	Jacobian matrix	α_r	pitch angle (rad)
J_{damped}	damped Jacobian matrix	α_θ	roll angle (rad)
k	iteration number	β	relative texture extend in radial direction
p	local pressure (Pa)	η	lubricant dynamic viscosity (Pa.s)
p_{cav}	cavitation pressure (Pa)	θ	circumferential coordinate (rad)
r	radial coordinate (m)	θ_p	circumferential coordinate of pivot (rad)
r_i	inner pad radius (m)	θ	fractional film content
r_o	outer pad radius (m)	ρ	lubricant density (kg/m^3)
r_p	radial coordinate of pivot (m)	ω	rotational speed (rpm)
S	relative texture depth		